**FULL PAPER**

Nanowire Phototransistor

ADVANCED
MATERIALS
INTERFACES

www.advmatinterfaces.de

# Enhanced Negative Photoconductivity in InAs Nanowire Phototransistors Surface-Modified with Molecular Monolayers

*Lifan Shen, SenPo Yip, Changyong Lan, Lei Shu, Dapan Li, Ziyao Zhou, Chun-Yuen Wong, Edwin Y. B. Pun,\* and Johnny C. Ho\**

Negative photoconductivity (NPC) mechanisms are widely investigated for high-performance InAs nanowire (NW) phototransistors, where these mechanisms are usually attributed to severe carrier scattering centers, light-assisted hot electron trapping in the surface oxide, and/or defects induced photogating layer. However, further insights into their photodetecting mechanisms, as well as corresponding performance enhancement of these NW phototransistors, are still very limited. This work reports the NPC behavior in surface-modified InAs NW phototransistors based on photoexcitation induced majority electron trapping in the bonded sulfur monolayer under optical illumination. In order to enhance hot electron trapping ability of the bonded sulfur layer, aromatic thiolate (ArS⁻)-based molecular monolayer with strong electron-withdrawing group is employed using simple wet chemistry for the surface modification of InAs NW phototransistors. The magnitude of the photoexcitation induced hot electron trapping is increased by the stronger electron-withdrawing ability of the ArS⁻-based molecular monolayer, enabling the hot electrons to be trapped and released more efficiently, resulting in NW phototransistors with good sensitivity, fast photoresponse, and long-term stability to low intensity visible light. These results confirm the potential of InAs NW phototransistors surface-passivated with molecular monolayers in the application and realization of high-sensitive and long-term stable room temperature nanoscale photodetectors.

## 1. Introduction

In recent years, III–V compound semiconductor nanowires (NWs) have been considered as promising active material candidates for next-generation flexible electronics, photonics, and sensors, due to their high carrier mobility, tunable direct bandgap, excellent mechanical flexibility, superior photoresponsibility, and extraordinarily large surface-to-volume ratio.[1–9] In particular, InAs NWs, having narrow direct bandgap, ultrahigh electron mobility, as well as room temperature highly efficient visible and near-infrared photoresponse, have been demonstrated in both electronic and optoelectronic applications, including broad-spectrum photodetectors covering the ultraviolet to infrared wavelength region.[10–14] However, significant quantities of surface charges are inevitably trapped on the NW surfaces, owing to the presence of large amounts of surface states originating from their unstable native oxide, forming an electron surface accumulation layer and resulting in a Fermi level pinning above the conduction band.

Dr. L. Shen, Prof. E. Y. B. Pun
Department of Electronic Engineering
City University of Hong Kong
83 Tat Chee Avenue, Kowloon, Hong Kong SAR, China
E-mail: eeeybpun@cityu.edu.hk
Dr. L. Shen, S. Yip, Dr. C. Lan, Z. Zhou, Dr. C.-Y. Wong,
Prof. E. Y. B. Pun, Dr. J. C. Ho
State Key Laboratory of Millimeter Waves
City University of Hong Kong
83 Tat Chee Avenue, Kowloon, Hong Kong SAR, China
E-mail: johnnyho@cityu.edu.hk
S. Yip, Dr. C. Lan, L. Shu, D. Li, Z. Zhou, Dr. J. C. Ho
Department of Materials Science and Engineering
City University of Hong Kong
83 Tat Chee Avenue, Kowloon, Hong Kong SAR, China

S. Yip, Dr. C. Lan, L. Shu, D. Li, Z. Zhou, Dr. J. C. Ho
Centre of Functional Photonics
City University of Hong Kong
83 Tat Chee Avenue, Kowloon, Hong Kong SAR, China
S. Yip, L. Shu, D. Li, Z. Zhou, Dr. C.-Y. Wong, Dr. J. C. Ho
Shenzhen Research Institute
City University of Hong Kong
Shenzhen 518057, China
Dr. C.-Y. Wong
Department of Chemistry
City University of Hong Kong
83 Tat Chee Avenue, Kowloon, Hong Kong SAR, China

**ADVANCED
SCIENCE NEWS**
www.advancedsciencenews.com

**ADVANCED
MATERIALS
INTERFACES**
www.advmatinterfaces.de

This pinning is notoriously known to degrade the chemical and physical properties of NWs;[15–17] thus, in order to facilitate practical utilizations of InAs NWs, it is essential to manipulate these surface states. This can be achieved using, for example, surface passivation or modification of III–V NWs by self-assembled sulfur-containing monolayer (SAM) and ammonium sulfide $(NH_4)_2S$, which have been commonly employed to enhance NW transistor performances in different fabrication schemes.[18,19] Aromatic thiolate $(ArS^-)$-based molecular monolayers have also been proved to be efficient in modulating the electron transport properties of InAs NWs, such as controlling the device operation mode.[20] Nevertheless, reports focusing on the photoresponsivity and corresponding mechanism of InAs NW surface-modified with molecular monolayers are still limited, and it is important to understand and have further insights on all these phenomenon in order to enhance the photosensing performance of NW based optoelectronic devices.

Two different photodetecting mechanisms have been widely investigated for single InAs NW photodetector: positive photoconductivity (PPC) and negative photoconductivity (NPC). In PPC, the conductivity of InAs NWs increases with incident irradiation because the photoexcitation injects additional charge carriers. On the other hand, several competing mechanisms have been observed in NPC. NPC is a majority-carrier-dominated photodetecting mechanism, equipped with a self-assembled photogating layer (PGL) trapping photogenerated electrons and leaving the unpaired holes to recombine with the NW carriers, and the current reduces under light illumination.[21] It can also be attributed to the enhanced carrier scattering by trapping photoelectrons in the oxide layer, as evidenced by a reduced carrier mobility under light illumination,[22] or due to the depletion of conduction channels by light assisted hot electron trapping.[23] In this work, we employ molecular monolayers to modify the InAs NW surfaces, study and clarify the corresponding NPC behaviors for the first time. It is found that the origin of NPC can be ascribed to the photoexcitation induced majority electron trapping in the bonded monolayer (i.e., sulfur (S)), which leads to a decrease in the photocurrent under 635nm wavelength laser illumination. To further enhance the hot electron trapping ability of the bonded S layer, $ArS^-$-based molecular monolayer with stronger electron-withdrawing group is adopted for the surface modification of the InAs NW phototransistors by simple wet chemistry. The stronger electron-withdrawing ability of the $ArS^-$-based molecular monolayers not only increases the photoexcitation induced hot electron trapping magnitude, it also enables the hot electrons to be efficiently trapped and released, resulting in passivated InAs NW phototransistors having good sensitivities, fast photoresponses, and long-term stabilities to low power visible light illumination. The results demonstrate the effectiveness of utilizing molecular monolayer modification to enhance NPC effect in InAs NWs for high-sensitive broad-spectrum photodetection.

## 2. Results and Discussion

### 2.1. Negative Photoconductivity in InAs NW Phototransistors with Surface Modification of $(NH_4)_2S$

Scanning electron microscope (SEM) and transmission electron microscopy (TEM) images of the as-grown InAs NWs, synthesized by the catalytic chemical vapor deposition (CVD) method in this work, are shown in **Figure 1**a,b. The NWs are straight, long, and dense with a uniform diameter along their entire length. In order to evaluate the crystallinity of the obtained NWs, high-resolution TEM (HRTEM) is performed and a typical HRTEM image is shown in Figure 1c. Based on the plane spacing determination and the reciprocal lattice spots extracted by fast Fourier transform (FFT), the NW exhibits single-crystalline zinc-blended crystal structure with a dominant growth orientation in the ⟨110⟩ direction. Also, there is no significant amount of stacking faults or twin-plane polytypic defects observed on the NW sample. As demonstrated in previous work, there is a thin layer of native oxide (≈3 nm) on the NW surface.[24] SEM image of the top view of a representative InAs NW phototransistor is shown in Figure 1d. The phototransistor consists of a single InAs NW as the channel material with a diameter $d ≈ 35$ nm and a channel length of $L ≈ 4.51$ µm.

The transfer characteristics (i.e., $I_{DS}$–$V_{GS}$ curves) of the InAs NW transistor before and after $(NH_4)_2S$ passivation with $V_{DS} = 0.1$ V are shown in **Figure 2**a. It can be seen that after surface modification, both the on and off currents decrease, and the $I_{on}/I_{off}$ ratio increases to $2.34 × 10^4$. The magnitude of the hysteresis decreases as well as the threshold voltage $(V_{Th})$ shifts to the positive region for about 0.3 V. The corresponding output characteristics ($I_{DS}$–$V_{DS}$ curves) of the same InAs NW transistor are also measured before modification with and without light illumination (635 nm wavelength, 0.07 mW mm$^{-2}$) in ambient as depicted in Figure S1a (Supporting Information). The linear relationship between the $I_{DS}$ and $V_{DS}$ curves indicates the existence of Ohmic-like electrical contact with insignificant barrier. The current increases with increasing $V_{GS}$ (i.e., the back-gate voltage), which confirms that the NW has a typical n-type electrical characteristic. Also, there is no obvious change in the $I_{DS}$–$V_{DS}$ curves with and without laser illumination. The dark current is only slightly higher than that with laser illumination under higher $V_{DS}$, indicating that the photoresponse for the unpassivated InAs NW transistor under 0.07 mW mm$^{-2}$ light intensity is extremely weak. The photoresponse properties of the unpassivated NW transistor are also investigated by switching the incident light on and off at an interval of 5 s by a chopper with $V_{DS} = 0.1$ V and $V_G = -5$ V, as shown in Figure S1b (Supporting Information). There is almost no photoresponse for the unpassivated NW transistor, which further supports the $I_{DS}$–$V_{DS}$ results discussed above.

The photoresponse of the InAs NW transistor after $(NH_4)_2S$ surface passivation is measured under the same condition ($V_{DS} = 0.1$ V and $V_G = -5$ V) as shown in Figure 2b as black line. When the light is on, the light current ($I_{light}$) is recorded in a lower current (i.e., high resistive) state. When the light is off, the dark current ($I_{dark}$) is switched to a higher current (i.e., low resistive) state under dark condition. Hence, the photocurrent $I_{photo}$ ($I_{photo} = I_{light} - I_{dark}$) of the passivated InAs NW transistor exhibiting the NPC behavior can be determined. This NPC effect of the passivated NW transistor shows good stability and excellent reproducibility during the 635 nm wavelength laser light on/off cycles. In order to further evaluate the sensitivity of the $(NH_4)_2S$ passivated NW phototransistor, the photoresponse measurements under different light intensities (0.07, 0.14, 0.21, 0.42, 0.56, and 0.7 mW mm$^{-2}$) were carried
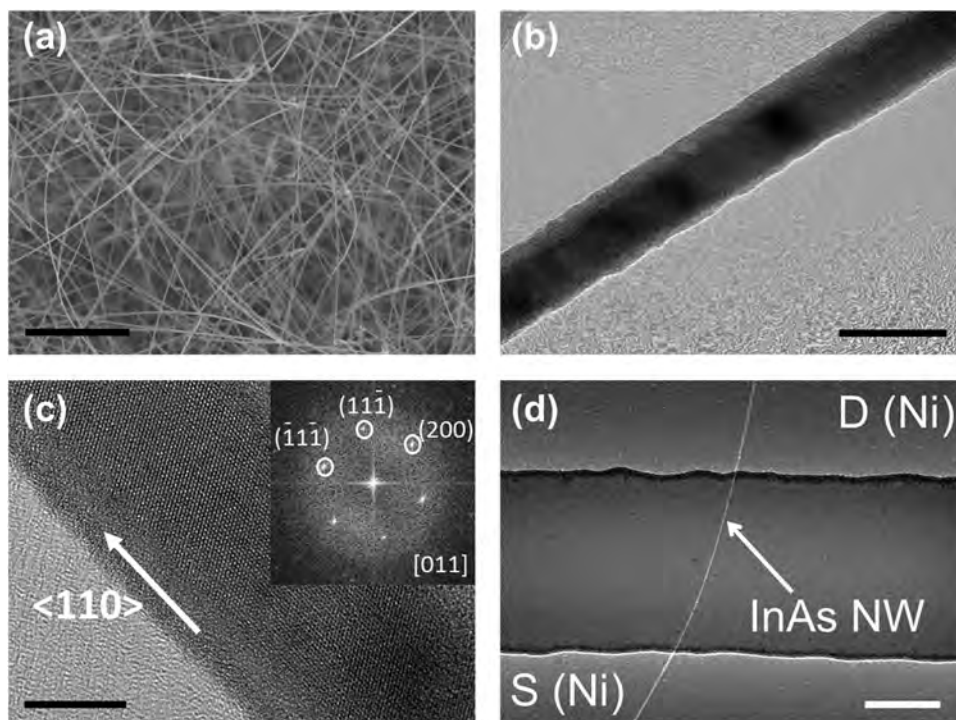
**Figure 1.** Characterization of InAs NWs. a) SEM image of the as-grown InAs NWs (scale bar, 2 μm). b) TEM image of a representative NW (scale bar, 50 nm). c) High-resolution TEM image and the corresponding fast Fourier transform (FFT) of a representative NW (scale bar, 10 nm). d) SEM image of the fabricated single InAs NW phototransistor (scale bar, 2 μm).
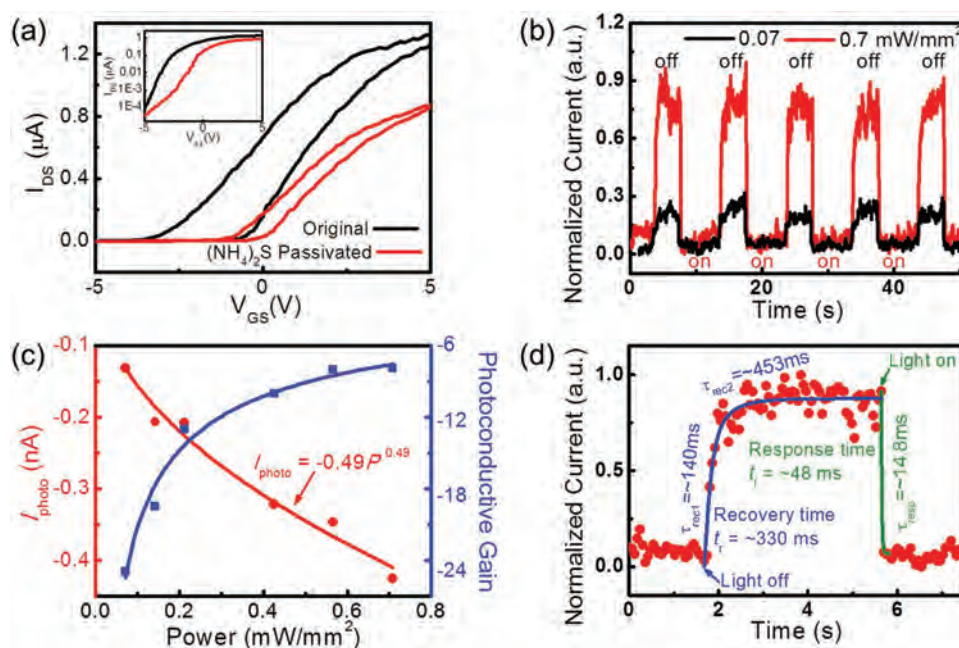


**Figure 2.** Photoresponse of the InAs NW photodetector surface-passivated with $(NH_4)_2S$ monolayer. a) Transfer characteristics of the InAs NW phototransistor before and after $(NH_4)_2S$ passivation (inset: in logarithmic scale) with $V_{DS} = 0.1$ V. b) Photoresponse characteristics of the InAs NW photodetector under modulated red laser illumination (635 nm wavelength) at different light intensities: 0.07 and 0.7 mW mm$^{-2}$ (the reference current for normalization is 0.51 nA). c) Photocurrent and photoconductive gain as a function of incident light intensity extracted from the data shown in Figure 2b and Figure S2 (Supporting Information). d) A single normalized modulation cycle measured with a light intensity of 0.07 mW cm$^{-2}$ (the reference current for normalization is 0.44 nA). For (b), (c), and (d), $V_{DS} = 0.1$ V and $V_G = -5$ V.

out with $V_{DS} = 0.1$ V and $V_G = -5$ V, as shown in Figure S2 (Supporting Information). The $I_{dark}$ increases with increasing light intensity. When the light intensity increases from 0.07 to 0.7 mW mm$^{-2}$, the photocurrent increases by about three times with $V_{DS} = 0.1$ V and $V_G = -5$ V, as shown in Figure 2b. The dependence of photocurrent ($I_{photo}$) on incident light intensity ($P$) can be simply fitted to a simple power law of $I_{photo} = AP^{\theta}$, where $A$ is a constant for a certain light wavelength, and the exponent $\theta$ determines the response of photocurrent to light intensity.[25–28] Fitting the data in Figure 2c, $\theta = 0.49$ is obtained. This noninteger power-law dependence ($\theta < 1$) of photocurrent on light intensity suggests a complex electron–hole recombination process via recombination centers and traps.[29,30] Due to the NPC effect, the negative $I_{photo}$ leads to a negative constant $A$. In addition, there are two key parameters for a photodetector, the responsivity ($R$) and the photogain ($G$), which reflect and quantify the sensitivity of a photodetector to the incident light. $R$ is defined as the photocurrent generated per unit of incident power, and can be represented by using the following equation: $R = (I_{light} - I_{dark})/P = I_{photo}/P_{opt}$, where $P_{opt}$ is the light power absorbed by the effective semiconductor conductive channel.[25,27] $G$ is defined as the number of charges collected by electrodes due to the excitation by one photon, and can be expressed as $G = (I_{photo}/P_{opt})(h\upsilon/q) = Rh\upsilon/q$, where $h\upsilon$ is the energy of an incident photon and $q$ is the electron charge.[31] The blue fitting curve in Figure 2c shows the calculated $G$ as a function of $P$ with $V_{DS} = 0.1$ V, $V_G = -5$ V. In order to compare our photodetectors with other NW photodetectors that usually have positive photoconductivity, we define the negative $G$ as the number of carriers that "cannot be collected" by the electrodes per incident photon. Hence, the only difference is that the gain is negative in our case. Assuming all the incident light on the channel is absorbed, a negative gain of around −24 is obtained when the light intensity is 0.07 mW mm$^{-2}$ with $V_{DS} = 0.1$ V and $V_G = -5$ V. When the light intensity increases, $G$ becomes more negative due mainly to the carrier-trap saturation effect. To show reproducibility, stability, and practical application of our passivated NW photodetectors, the devices were turned on and off by over 90 cycles and show no sign of degradation, as shown in Figure S3c (Supporting Information).

The phototransistor response speed is another key parameter, since it determines the capability of the device to follow fast-varying optical signals.[21,31] A single normalized modulation cycle of the NW phototransistor measured with a light intensity of 0.07 mW mm$^{-2}$ with $V_{DS} = 0.1$ V and $V_G = -5$ V is also shown in Figure 2d. The measured response time (i.e., falling time, $t_f$), defined as the time required for the current to decrease from 90% $I_{peak}$ to 10% $I_{peak}$, is <48 ms (limited by the minimum sampling interval value of our measurement system), and the recovery time (i.e., rising time, $t_r$) which is defined as the time for the current to increase from 10% to 90%, is ≈330 ms. The falling time is always shorter than the corresponding rising time, resulting in a nonsymmetric curve with different rising and falling edges. By fitting the rising and falling edges with the equations of $I = I_0[1 - A\exp(-t/\tau_{rec1}) - B\exp(-t/\tau_{rec2})]$ and $I = I_0[1 + C\exp(-t/\tau_{resp})]$, the time constants for recovery, $\tau_{rec1}$ and $\tau_{rec2}$, are obtained to be ≈140 and 453 ms, corresponding to the fast and slow recovery processes, respectively, and the time constant for response ($\tau_{resp}$) is ≈14.8 ms. Considering

the limitation of the minimum sampling interval value of our measurement system, the actual response times of the passivated NW devices should be shorter. The fastest response and recovery times have been measured to be ≈17.5 and ≈180 ms, respectively, under low laser light intensity of 0.045 mW mm$^{-2}$ as given in Figure S3d (Supporting Information). As compared with the reported response time of 12 ms and recovery time of 3.92 s with light intensity 8 mW mm$^{-2}$ at $V_G = 40$ V in InAs NW phototransistors induced by photogating layer,[21] the photoresponse speed of our surface-modified InAs NW phototransistor is fast even under a low light intensity of 0.045 mW mm$^{-2}$ and low power of $V_G = -5$ V, which confirms the excellent photosensing performances of the passivated NW phototransistors.

## 2.2. Photodetection Mechanism in InAs Nanowire Phototransistors with Molecular Monolayers

It has been reported that the NPC effect is caused by light-assisted hot electron trapping in the oxide layer and PGL, or severe carrier scattering in the charged recombination centers in III–V materials.[21–23] From our experimental measurements, the NPC mechanism in the $(NH_4)_2S$ passivated InAs NW phototransistor is shown schematically in **Figure 3**. Surface modification of III–V NWs by self-assembled sulfur-containing monolayer, such as $(NH_4)_2S$, is widely adopted in many applications, and the NW device performance is enhanced by improving the subthreshold slope (SS) and increasing the carrier mobility ($\mu_{FE}$).[18,19] It has also been reported that the $(NH_4)_2S$ modification can effectively remove the surface oxides and impurities with minimal surface etching, establishing a covalently bonded sulfur monolayer on the InAs NW surface with good stability in ambient air.[18,19,32] The enhancement of SS and $\mu_{FE}$ can be attributed to the reduction of InAs NW surface trap states and surface carrier scattering centers due to the saturated sulfur bond formation (S-bond). In our case, the sulfur binding established on the InAs NW surface via In−S and As−S linkages in the modified NW phototransistor is shown in Figure 3a. Before light illumination, the free electrons in the NW core are driven by the electric field and form the dark current. When the NW is exposed to 635 nm wavelength laser light, the photogating effect occurs in the bonded sulfur monolayer on the NW surface, which can be regarded as a PGL. This PGL traps the photoexcited electrons from the core and the photogenerated electron–hole pairs are separated, leaving the photogenerated holes to recombine with the free electrons in the core. All these would lead to a rapid decrease in the electron density in the core, resulting in a decreasing current (low $I_{light}$ or high resistive state) as shown in Figure 3b. Moreover, the trapped hot electrons in the PGL generate a built-in electric field, depleting the free electrons in the core and reducing further the photocurrent. When the laser light is turned off, the trapped electrons are released from the PGL to the core through a thermal process, resulting in high $I_{dark}$ (or low resistive state, as shown in Figure 3c). The recovery process consists of a fast recovery time followed by a slower tail, when the light is switched off as shown in Figure 2d (blue line) and Figure S3d (Supporting Information), indicating that the trapped charges are slowly released to the conduction band (CB).
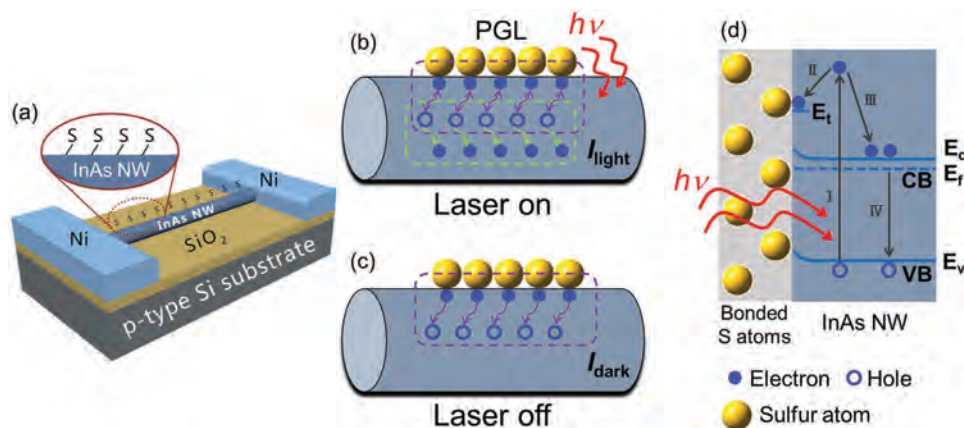
**Figure 3.** Schematic illustrations for the InAs NW phototransistor photoresponse mechanism. a) Schematic of the sulfur binding on the surface of the InAs nanowire (the field-effect transistor (FET) channel). b) The process of photogenerated electron–hole pairs separation under laser light and the photoexcited electrons being trapped by the PGL, leaving the photogenerated holes to recombine with the free electrons in the core. c) The process of trapped electrons being released from the PGL to the core after the laser light is switched off. d) Energy band diagram displaying the excitation (I), the trapping (II), the thermalization (III), and the recombination (IV) processes.

The transconductance of the modified InAs NW phototransistor remains almost the same with or without light illumination (Figure S3a, Supporting Information), this result is different from the previously reported NPC in InAs NWs and InN thin films where the carrier mobility is reduced under illumination due to the severe scattering in the charged recombination centers.[22,33] The energy band diagram, as shown in Figure 3d, further illustrates the photodetection mechanism of our passivated NW phototransistor with the PGL. When photons with energy much higher than the bandgap of InAs NWs incident on the phototransistor, the photogenerated hot electrons can overcome the barrier and get trapped in the bonded sulfur layer, corresponding to the processes I and II, as shown in Figure 3d. The trapped electrons would then reduce the electron density in the CB and the photogenerated holes would immediately recombine with the free electrons in the NW core, resulting in a rapid decrease of the photocurrent corresponding to the fast response process as shown in Figure 2d (green line). When the incident light is switched off, the trapped electrons are released back to the CB over the energy barrier through a thermal activation process III as shown in Figure 3d, or further recombine with holes in the valence band (VB) (process IV). Hence, the photosuppressed conductance recovers following the recovery process as described in Figure 2d (blue line). When the phototransistor is illuminated with higher incident light intensity (Figure 2b), more photogenerated hot electrons are trapped in the PGL. When the light is turned off, this trapping would result in additional trapped electrons being released from the PGL to the NW core and contributing to a higher $I_{dark}$.

### 2.3. Enhanced Negative Photoconductivity with ArS⁻-Based Molecular Monolayers

In order to verify the NPC mechanism and to enhance further the hot electron trapping ability of the PGL, aromatic thiolate (ArS⁻)-based molecular monolayer with stronger electron-withdrawing group is employed for the surface modification of InAs NW phototransistor by simple wet chemistry. The ArS⁻-based molecular monolayer has been proven to be an effective surface modifier with controllable electron density at the linkage established between the modifier and the NW surface, improving the NW carrier mobility by passivating the surface state and modulating the device $V_{Th}$ by varying the electron density of the modifier.[20] For the SAM formation, the InAs NWs were pretreated with 1% hydrofluoric acid (HF) under nitrogen atmosphere to remove the native surface oxide and to avoid reoxidation. To further minimize the solvent binding onto the NW surface, isopropyl alcohol (IPA), a branched alcohol, is chosen as the solvent for the aromatic thiol (ArSH) solution. The p-fluorothiophenol (F–C₆H₄SH) modification is then adopted here due to its stronger electron-withdrawing ability of the substituent, which is found to lead to a larger $V_{Th}$ shift to the positive region.[20] After passivation, the ArS⁻ groups are confirmed to bind onto the NW surface by both the In—S and As—S linkages, which are similar to the bonded sulfur monolayer acting as the PGL as described in Figure 3a.[20] The transfer characteristics of the InAs NW transistor before and after F–C₆H₄SH passivation measured with $V_{DS} = 0.1$ V are shown in **Figure 4**a. After modification, the device $V_{Th}$ shifts to the positive region with a value of ≈1.3 V due to the stronger electron-withdrawing effect of the ArS⁻ group. Moreover, the NW phototransistors remain operating in an Ohmic-like behavior as confirmed by the output characteristics ($I_{DS}$–$V_{DS}$ curves), as shown in Figure S4a (Supporting Information). The results suggest that the passivation process does not induce any adverse effect on the electrical contact properties of the NW phototransistor. The photoresponse of the InAs NW phototransistor is also investigated before passivation with modulated laser light (635 nm, 0.07 mW mm⁻²) with $V_{DS} = 0.1$ V and $V_G = -5$ V (Figure S4b, Supporting Information). There is no noticeable photoresponse for the unmodified or unpassivated NW transistor. After ArS⁻ passivation, the photocurrent responses of the treated InAs NW transistor under the same condition are shown in Figure 4b as black line. NPC behavior is
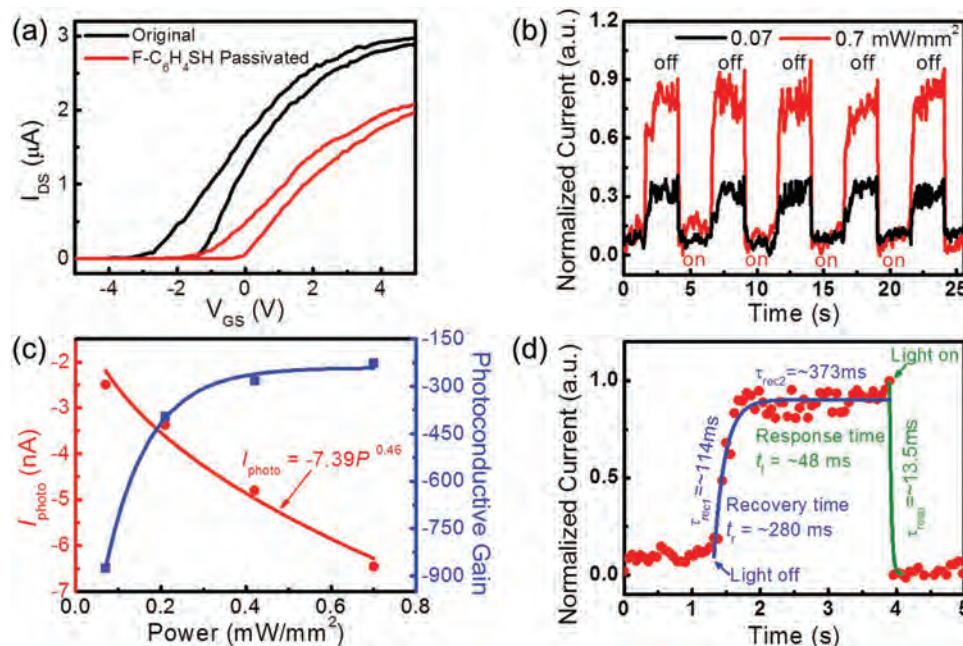
**Figure 4.** Photoresponse of the InAs NW photodetector surface modified with F–$C_6H_4$SH passivation. a) Transfer characteristics of the InAs phototransistor before and after the F–$C_6H_4$SH passivation with $V_{DS} = 0.1$ V. b) Photoresponse characteristics of the InAs NW photodetector under modulated red laser illumination (635 nm wavelength) at different light intensities: 0.07 and 0.7 mW mm$^{-2}$ (the reference current for normalization is 0.76 nA). c) Photocurrent and photoconductive gain as a function of incident light intensity extracted from the data shown in Figure 4b and Figure S5 (Supporting Information). d) A single normalized modulation cycle measured with a light intensity of 0.07 mW cm$^{-2}$ (the reference current for normalization is 0.63 nA). For both (b) and (d), $V_{DS} = 0.1$ V and $V_G = -5$ V.

also observed in the F–$C_6H_4$SH passivated InAs NW phototransistors under low laser light intensity. The photoresponse measurements under different light intensities (0.07, 0.21, 0.42, and 0.7 mW mm$^{-2}$) were carried out, as shown in Figure S5 (Supporting Information). Similar to the previous discussion, the $I_{dark}$ improves with increasing light intensity, and the photocurrent increases by about three times when the light intensity increases from 0.07 to 0.7 mW mm$^{-2}$ with $V_{DS} = 0.1$ V and $V_G = -5$ V, as shown in Figure 4b. The dependence of $I_{photo}$ on $P$ can be fitted by a noninteger power-law with $\theta = 0.46$, as shown by the red curve in Figure 4c. $R$ and $G$ are also calculated as a function of $P$, and fitted by the blue curve as shown in Figure 4c. A high negative gain of around −880 is obtained under a light intensity of 0.07 mW mm$^{-2}$ with $V_{DS} = 0.1$ V and $V_G = -5$ V, and this value is much larger than that of $(NH_4)_2$S modified phototransistor, indicating the effectiveness of the ArS$^-$-based molecular monolayer modification and a good sensitivity of the F–$C_6H_4$SH passivated InAs NW phototransistors to the low intensity light irradiation. For the photoresponse speed evaluation, a single normalized modulation cycle is measured using a light intensity of 0.07 mW mm$^{-2}$ with $V_{DS} = 0.1$ V and $V_G = -5$ V, as shown in Figure 4d. Due to the limitation of the minimum sampling interval value of our measurement system, the measured response time is found to be less than 48 ms and the recovery time is ≈280 ms. By fitting the rising and falling edges, the time constants $\tau_{rec1}$ and $\tau_{rec2}$ are found to be ≈114 and 373 ms, respectively, and $\tau_{resp}$ is ≈13.5 ms, which is comparable to the state-of-the-art InAs NW phototransistors operated even at the much higher gate power supply and light intensity.[21] The stronger electron-withdrawing ability of the ArS$^-$-based

molecular monolayer increases the photoexcitation induced hot electron trapping amount, enabling the hot electrons to be trapped and released in a faster manner, resulting in the F–$C_6H_4$SH passivated NW phototransistors exhibiting higher sensitivity and faster photoresponse to low power visible light. It is also noted that another ArS$^-$-based derivative, p-nitrothiophenol ($NO_2$–$C_6H_4$SH), with the stronger electron-withdrawing ability as compared with the one of F–$C_6H_4$SH is further employed to confirm the NPC mechanism here. Evidently, a higher current on/off ratio is obtained in the corresponding photoresponse of surface-modified NWs since $NO_2$–$C_6H_4$SH is anticipated to have the stronger electron-withdrawing ability than F–$C_6H_4$SH (Figure S6, Supporting Information).[20] More importantly, the effect of F–$C_6H_4$SH molecular monolayers on the electrical and photoresponse properties of NW phototransistors remains the same after 4 months of storage, confirming the long-term stability of the ArS$^-$-based monolayer passivated InAs NW phototransistors and their suitability for practical device applications.

## 3. Conclusions

In summary, we have demonstrated NPC behavior in molecular monolayer surface-passivated InAs NW phototransistors, and showed that the effect is due to the photoexcitation induced majority electron trapping in the bonded sulfur layer. In order to further enhance the hot electron trapping ability of the bonded sulfur layer, ArS$^-$-based molecular monolayer with stronger electron-withdrawing group is then used for the

surface modification of InAs NW phototransistor by simple wet chemistry. This stronger electron-withdrawing ability of the monolayers increases the photoexcitation induced hot electron trapping amount, enabling the hot electrons to be trapped and released more effectively, resulting in surface-modified InAs NW phototransistors having higher sensitivity, faster photoresponse, and long-term stability to low power visible light. The results confirm the suitability and application of InAs NW phototransistors modified with molecular monolayers as room temperature nanoscale photodetectors.

## 4. Experimental Section

*Nanowire Synthesis*: The InAs NWs used in this study were synthesized in a two-zone horizontal tube furnace using a solid-source CVD transport method as previously reported.[24] 0.2 nm thick of Ni film acting as catalyst was thermally evaporated onto $SiO_2/Si$ substrate (50 nm thick of thermal oxide grown on degenerately doped Si). The substrate was then positioned in the downstream zone of the furnace. About 1.2 g of InAs powder (99.9999% purity) was placed inside a boron nitride crucible placed in the upstream zone and heated to 690 °C. Hydrogen (99.9995%, 200 sccm) was used to carry the evaporated precursors to the downstream zone heated to a temperature of 470 °C. The InAs NWs were grown for 60 min utilizing the Ni catalyst which was preannealed at 800 °C for 10 min, and the pressure was maintained at ≈1.0 Torr. After the CVD growth, the source and substrate heaters were stopped together and the system was allowed to cool down to room temperature under hydrogen flow before the grown NWs were taken out of the furnace.

*Material Characterizations*: In order to establish a consistent study, all material characterizations were performed on NWs grown within the front 1 cm region of the growth substrates. Surface morphologies of the grown NWs were examined with a SEM (FEI/Philips XL30 ESEM-FEG). TEM and HRTEM images were observed with a JEOL 2100F transmission electron microscope.

*Nanowire Phototransistor Fabrication and Measurements*: The CVD grown InAs NWs were harvested in anhydrous ethanol by sonication and then drop-casted onto $SiO_2/Si$ substrates for the fabrication of back-gated FETs. The electrodes of the phototransistors were defined using a standard lithography process, followed by deposition of 50 nm thick of Ni metal and lift off process. A 10 s HF (1%) etch was applied prior to the Ni metal deposition in order to remove the NW native oxide and ensure the formation of Ohmic-like contact between the metal electrode and the NW channel. The optoelectronic properties of the fabricated devices were characterized using a standard electrical probe station and an Agilent 4155C semiconductor parameter analyzer at room temperature. A 635 nm laser was used as light source for photodetection measurements. The power of the light was tuned by an attenuator and was measured by a power meter (PM400, Thorlabs USA). A homemade mechanical chopper was used to modulate the incident light.

*Surface Modification by Self-Assembly of Monolayer*: The surface passivation of InAs NWs after device fabrication was prepared under $N_2$ atmosphere using the procedures as previously reported.[20] For the p-fluorothiophenol (F–$C_6H_4$SH) modification, the fabricated devices were first pretreated with 1% HF solution under nitrogen atmosphere for 6 s, rinsed by deionized water, and then placed into the freshly prepared $35 \times 10^{-3}$ M IPA solution of F–$C_6H_4$SH at room temperature for 12 h. The device wafers were removed from the IPA solution, rinsed with ethanol, and blown dried with nitrogen. For the p-nitrothiophenol ($NO_2$–$C_6H_4$SH) modification, the devices were first pretreated with 1% HF solution under nitrogen atmosphere for 6 s, rinsed by deionized water, and then placed into the freshly prepared $35 \times 10^{-3}$ M toluene solution of $NO_2$—$C_6H_4$SH at room temperature for 12 h. Here, the solvent is replaced with toluene, since $NO_2$—$C_6H_4$SH cannot be dissolved well in IPA. After being removed from the toluene solution, the device wafers were rinsed with ethanol and blown dried with nitrogen.

For the $(NH_4)_2$S passivation, the devices were soaked in $(NH_4)_2$S solution (stock solution) for 40 s in order to passivate the NW surfaces. After passivation, the devices were rinsed carefully using deionized water and ethanol and baked at 120 °C for ≈5 h.

## Supporting Information

Supporting Information is available from the Wiley Online Library or from the author.

## Conflict of Interest

The authors declare no conflict of interest.

[1] J. Wallentin, N. Anttu, D. Asoli, M. Huffman, I. Åberg, M. H. Magnusson, G. Siefer, P. Fuss-Kailuweit, F. Dimroth, B. Witzigmann, *Science* **2013**, *339*, 1057.

[2] Z.-x. Yang, N. Han, M. Fang, H. Lin, H.-Y. Cheung, S. Yip, E.-J. Wang, T. Hung, C.-Y. Wong, J. C. Ho, *Nat. Commun.* **2014**, *5*, 5249.

[3] D. Saxena, S. Mokkapati, P. Parkinson, N. Jiang, Q. Gao, H. H. Tan, C. Jagadish, *Nat. Photonics* **2013**, *7*, 963.

[4] Z. Fan, J. C. Ho, T. Takahashi, R. Yerushalmi, K. Takei, A. C. Ford, Y. L. Chueh, A. Javey, *Adv. Mater.* **2009**, *21*, 3730.

[5] T. Takahashi, K. Takei, J. C. Ho, Y.-L. Chueh, Z. Fan, A. Javey, *J. Am. Chem. Soc.* **2009**, *131*, 2102.

[6] A. C. Ford, J. C. Ho, Z. Fan, O. Ergen, V. Altoe, S. Aloni, H. Razavi, A. Javey, *Nano Res.* **2008**, *1*, 32.

[7] Y.-Z. Long, M. Yu, B. Sun, C.-Z. Gu, Z. Fan, *Chem. Soc. Rev.* **2012**, *41*, 4560.

[8] S. Ju, A. Facchetti, Y. Xuan, J. Liu, F. Ishikawa, P. Ye, C. Zhou, T. J. Marks, D. B. Janes, *Nat. Nanotechnol.* **2007**, *2*, 378.

[9] D. Zheng, J. Wang, W. Hu, L. Liao, H. Fang, N. Guo, P. Wang, F. Gong, X. Wang, Z. Fan, *Nano Lett.* **2016**, *16*, 2548.

[10] W. Wei, X.-Y. Bao, C. Soci, Y. Ding, Z.-L. Wang, D. Wang, *Nano Lett.* **2009**, *9*, 2926.

[11] J. Miao, W. Hu, N. Guo, Z. Lu, X. Liu, L. Liao, P. Chen, T. Jiang, S. Wu, J. C. Ho, *Small* **2015**, *11*, 936.

[12] Z. Liu, T. Luo, B. Liang, G. Chen, G. Yu, X. Xie, D. Chen, G. Shen, *Nano Res.* **2013**, *6*, 775.

[13] H. W. Shin, S. J. Lee, D. G. Kim, M.-H. Bae, J. Heo, K. J. Choi, W. J. Choi, J.-w. Choe, J. C. Shin, *Sci. Rep.* **2015**, *5*, 10764.

[14] T. Takahashi, K. Takei, E. Adabi, Z. Fan, A. M. Niknejad, A. Javey, *ACS Nano* **2010**, *4*, 5855.

[15] C. Thelander, M. Björk, M. Larsson, A. Hansen, L. Wallenberg, L. Samuelson, *Solid State Commun.* **2004**, *131*, 573.

[16] Q. L. Hang, F. D. Wang, P. D. Carpenter, D. Zemlyanov, D. Zakharov, E. A. Stach, W. E. Buhro, D. B. Janes, *Nano Lett.* **2008**, *8*, 49.

[17] S. A. Dayeh, D. P. Aplin, X. Zhou, P. K. Yu, E. T. Yu, D. Wang, *Small* **2007**, *3*, 326.

[18] D. Y. Petrovykh, M. J. Yang, L. J. Whitman, *Surf. Sci.* **2003**, *523*, 231.

[19] Q. Hang, F. Wang, P. D. Carpenter, D. Zemlyanov, D. Zakharov, E. A. Stach, W. E. Buhro, D. B. Janes, *Nano Lett.* **2008**, *8*, 49.

[20] H.-Y. Cheung, S. Yip, N. Han, G. Dong, M. Fang, Z.-x. Yang, F. Wang, H. Lin, C.-Y. Wong, J. C. Ho, *ACS Nano* **2015**, *9*, 7545.

[21] N. Guo, W. Hu, L. Liao, S. Yip, J. C. Ho, J. Miao, Z. Zhang, J. Zou, T. Jiang, S. Wu, *Adv. Mater.* **2014**, *26*, 8203.

[22] Y. Han, M. Fu, Z. Tang, X. Zheng, X. Ji, X. Wang, W. Lin, T. Yang, Q. Chen, *ACS Appl. Mater. Interfaces* **2017**, *9*, 2867.

[23] Y. Yang, X. Peng, H.-S. Kim, T. Kim, S. Jeon, H. K. Kang, W. Choi, J. Song, Y.-J. Doh, D. Yu, *Nano Lett.* **2015**, *15*, 5875.

[24] F. Wang, S. Yip, N. Han, K. Fok, H. Lin, J. J. Hou, G. Dong, T. Hung, K. Chan, J. C. Ho, *Nanotechnology* **2013**, *24*, 375202.

[25] C. Xie, F. Li, L. Zeng, L. Luo, L. Wang, C. Wu, J. Jie, *J. Mater. Chem. C* **2015**, *3*, 6307.

[26] S.-C. Kung, W. E. van der Veer, F. Yang, K. C. Donavan, R. M. Penner, *Nano Lett.* **2010**, *10*, 1481.

[27] D. Wu, Y. Jiang, Y. Zhang, J. Li, Y. Yu, Y. Zhang, Z. Zhu, L. Wang, C. Wu, L. Luo, *J. Mater. Chem.* **2012**, *22*, 6206.

[28] J. Jie, W. Zhang, Y. Jiang, X. Meng, Y. Li, S. Lee, *Nano Lett.* **2006**, *6*, 1887.

[29] A. Rose, *Concepts in Photoconductivity and Allied Problems*, Interscience Publishers Wiley, London **1963**.

[30] Y. Cao, Z. Liu, L. Chen, Y. Tang, L. Luo, J. Jie, W. Zhang, S. T. Lee, C. S. Lee, *Opt. Express* **2011**, *19*, 6100.

[31] P. Wu, Y. Dai, Y. Ye, Y. Yin, L. Dai, *J. Mater. Chem.* **2011**, *21*, 2563.

[32] N. Tajik, Z. Peng, P. Kuyanov, R. LaPierre, *Nanotechnology* **2011**, *22*, 225402.

[33] P.-C. Wei, S. Chattopadhyay, M.-D. Yang, S.-C. Tong, J.-L. Shen, C.-Y. Lu, H.-C. Shih, L.-C. Chen, K.-H. Chen, *Phys. Rev. B* **2010**, *81*, 045306.